Quantum dynamics for a fractal spectrum - Applications to simple processes in electrodynamics and quantum optics

Ariane SORET[1]

supervised by Eric AKKERMANS[2]

[1]ENS Cachan, France ; [2] Technion - Israel Institute of Technology, Haifa, Israel

September 2014 - July 2015

Contents

1   Introduction

During the past decades, there has been a growing interest for Schroedinger operators $H = -\frac{\hbar^2}{2m}\Delta + V(\mathbf{r})$ with an associated fractal spectrum. In fact, while the dynamics and the transport properties of quantum systems having a continuous or discrete spectrum are well understood, little is known about singular continuous spectra (like fractals), which are ubiquitous (quasi-crystals, quasi-periodic potentials, some glasses).

Some recent experiments [1], pursued at the Laboratoire de Photonique et Nanostructure (CNRS, Marcoussis, France) in partnership with my group at the Technion, on cavity polaritons placed in a quasi-periodic potential (which we will now refer to as "Fibonacci potential") with an associated Cantor like spectrum (we shall give a definition later), have evidenced a log-periodic behaviour for some dynamical quantities of the system. Although expected theoretically in the case of a fractal spectrum, such log-periodic oscillations had never been observed experimentally before.

With these experiments as a starting point, the objective of my internship was to understand, in the case of a triadic Cantor set spectrum (a type of fractal), how the fractal feature of the spectrum affects the dynamics and the propagation properties of the system, to determine which relevant physical quantities carry its signature, and to derive the analytical expression of those quantities. This study should then allow us to conduct further experiments.

After giving some generalities on fractals and the mathematical prerequisites, we will show that the structure of the spectrum translates in terms of a typical behaviour of relevant dynamical quantities - namely a power law with a characteristic exponent modulated by log-periodic oscillations. To illustrate this, we will derive the analytical expression of the time-averaged return probability $C(t) = \frac{1}{t}\int_0^t |\langle\psi(0)|\psi(t')\rangle|^2 dt'$ and show that its asymptotic expression has the form :

$$C(t) =_{t\to\infty} \left(\frac{t}{\tau}\right)^{-d_K} g(\ln(t/\tau))$$

where $d_K = \frac{\ln(2)}{\ln(3)}$ is the fractal dimension [2] of the triadic Cantor set, τ a time scale a g a periodic function which we calculate exactly. Then, we shall narrow our study to the tight-binding model; we show that in this case, the eigenfunctions can be seen as polynomials of the energy, and that the dynamics depend essentially on the Fourier transform (on a Cantor set) of monomes : $h_k(t) = \int_K e^{-ixt}x^k d\mu$, $k \in \mathbb{Z}$. This result enables us to study the dynamics of the system more thoroughly. As examples we consider two other relevant quantities, the root mean displacement $\Delta x(t) = \sqrt{\sum_k k^2|\psi(k,t)|^2}$, and the participation ratio, $P_r(t) = \frac{1}{\sum_k |\psi(k,t)|^4}$. We will then give some research perspectives.

2   Fractals, discrete scaling symmetry and Mellin transform

2.1   Definition and basic properties of fractals

It is difficult to give a concise and precise definition of a fractal. The term "fractal" (from latin *fractus*, "broken") was introduced by Mandelbrot to define objects too complicated to be treated in the frame of classical euclidean geometry :[1]: "*a fractal is a shape made of parts similar to the whole in some way*". We consider here fractals having a discrete scaling symmetry : if we zoom in on a specific zone, we find, in the same proportions, the initial shape.

As an example, let us consider the "Sierpinski gasket". Starting with an equilateral triangle, draw a line between the centers of the edges and remove the small triangle formed in the middle. By iterating this procedure an infinite number of times, we obtain a shape verifying a scaling property : if we zoom on one of the sub-triangles, we still see the same shape (fig. 1.a).

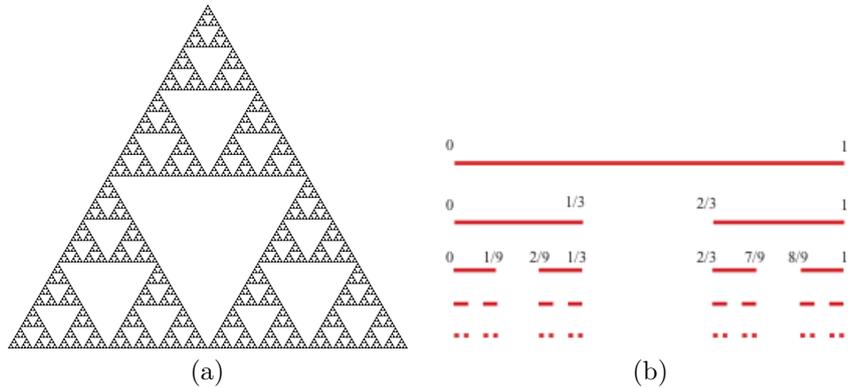
[1]Mandelbrot, correspondance, 1987

Figure 1: (a) Sierpinski gasket (source : commons.wikimedia.org). (b) Construction of a triadic Cantor set (accromath.uqam.ca).

2.2 Triadic Cantor set

Another classic example of a fractal is the triadic Cantor set, on which I have been working (fig. 1.b). Starting with the segment $[0, 1]$, divide it in three equal segments and remove the central one, and repeat the process on the two remaining segments. After an infinite number of steps, we obtain a set of isolated points, and of Lebesgue measure zero.

In this report, we note the triadic Cantor set K.

2.3 Fractal dimension

Intuitively, the dimension of a space or of a geometrical object can be understood as the (positive) number d such that a unit volume v has the form : $v = l^d$, where l is a length in the euclidean sense.

Fractals usually have non integer dimensions [2], which has deep consequences on the physical properties of systems presenting a fractal structure ([3], for a review [4]).

The triadic Cantor set, for instance, is of dimension $d_K = \frac{\ln(2)}{\ln(3)}$.

2.4 Discrete scaling property and log-periodic oscillations

We present here the mathematical method which will be used in order to study the connection between a fractal spectral feature and dynamical properties of a quantum system.

We consider here fractals with a scaling symmetry.

Mathematically, a function f displays a scaling symmetry if it verifies the functional equation :

$$f(x) = \frac{1}{b} f(ax)$$

for some real numbers (a, b), $b \neq 0$. If the set of real numbers (a, b) for which this equality holds is discrete, the function has a discrete scaling symmetry. In both cases, this property implies that the function f is of the form

$$f(x) = x^{\ln(b)/\ln(a)} g\left(\frac{\ln(x)}{\ln(a)}\right)$$

with g a periodic function of period 1 : $g(x + 1) = g(x)$ (the proof is given in the appendix).

In the case of a discrete scaling symmetry, the log-periodic function is usually not constant ; this specific behaviour (a log-periodic feature) is therefore the fingerprint of a fractal structure, which we will be looking for in measurable physical quantities.

Moreover, using Mellin transform, one can show that functions f verifying a relation of the form :

$$f(x) = \frac{1}{b} f(ax) + g(x)$$

4

may, under certain conditions on g, have the asymptotic form :

$$f(x) = x^{\ln(b)/\ln(a)} G\left(\frac{\ln x}{\ln a}\right)$$

with G 1-periodic. We shall give an example later, since the time-averaged return probability $C(t)$ is such a function.

3 Quantum dynamics for a triadic Cantor set spectrum

We now consider a one dimensional quantum system described by the state vector $|\psi(t)\rangle$ and evolving with the Hamiltonian $H = -\frac{\hbar^2}{2m}\frac{d^2}{dx^2} + V(x)$. We assume that the energy spectrum of H is a triadic Cantor set.

The system is initially in a state described by $|\psi(t=0)\rangle = |\psi_0\rangle$. After a time t, the state vector $|\psi(t)\rangle$ is given by :

$$|\psi(t)\rangle = e^{-i\hat{H}t/\hbar}|\psi_0\rangle$$

We shall also use the spectral decomposition of $|\psi(t)\rangle$ over an orthonormal basis of eigenfunctions $\{|\phi(\epsilon)\rangle\}$ of H, $|\phi(\epsilon)\rangle$ being the eigenfunction associated with the energy ϵ :

$$|\psi(t)\rangle = \int_{spectrum} g(\epsilon)e^{-i\epsilon t/\hbar}|\phi(\epsilon)\rangle d\tilde{\mu}(\epsilon)$$

where $g(\epsilon)$ is the projection of $|\psi_0\rangle$ on $|\phi(\epsilon)\rangle$, and $d\tilde{\mu}$ a measure defined on the spectrum. To alleviate the notations, we set $\hbar = 1$.

To go further, we need to define an appropriate measure on the spectrum. The triadic Cantor set K has a zero Lebesgue measure. However, in our case, the integrated density of states, e.g. the integral of the density of states $\rho(\epsilon)$ over the spectrum K, is non zero. Thus, $\rho(\epsilon)$ must be infinite in every point of K.

We define a measure $d\mu$ on K which takes into account the density of states : $d\mu(\epsilon) \equiv \rho(\epsilon)d\epsilon$. We proceed in the following way : we suppose that the density of states is uniform, and that the integrated density of states, $\mathcal{N}(\epsilon) = \int_K \theta(\epsilon - \epsilon')d\mu(\epsilon')$ with θ the Heaviside function, is bounded. Without loss of generality, we impose : $\int_K d\mu(\epsilon) = 1$. We then proceed iteratively : starting from a segment $[0,1]$, we set $\rho(\epsilon) = 1$ everywhere ; the integral thus equals 1. Now, divide the segment in three, remove the central part and define $\rho(\epsilon)$ to be equal to $\frac{3}{2}$ on $[0,\frac{1}{3}]$ and $[\frac{2}{3},1]$, and null on $[\frac{1}{3},\frac{2}{3}]$. We still have : $\int_0^1 \rho(x)dx = 1$. We repeat this process infinitely, and thus define $d\mu$ as a limit : for any function f defined on $[0,1]$, the integral of f over K is :

$$\int_K f(x)d\mu(x) = \lim_{n\to\infty}\left(\frac{3}{2}\right)^n \sum_{a_{j_n}\in P_n}\int_{a_{j_n}}^{a_{j_n}+3^{-n}} f(x)dx$$

where $\{P_n\}$ is the set of the left edges of the remaining segments after n iterations in the construction of the Cantor set.

One can show (see annexe) that $d\mu$ verifies the following important property :

$$\int_K f(x)d\mu(x) = \frac{1}{2}\int_K f\left(\frac{x}{3}\right)d\mu(x) + \frac{1}{2}\int_K f\left(\frac{x+2}{3}\right)d\mu(x) \tag{1}$$

This property still holds for multiple integrals ; it becomes, for a double integral :
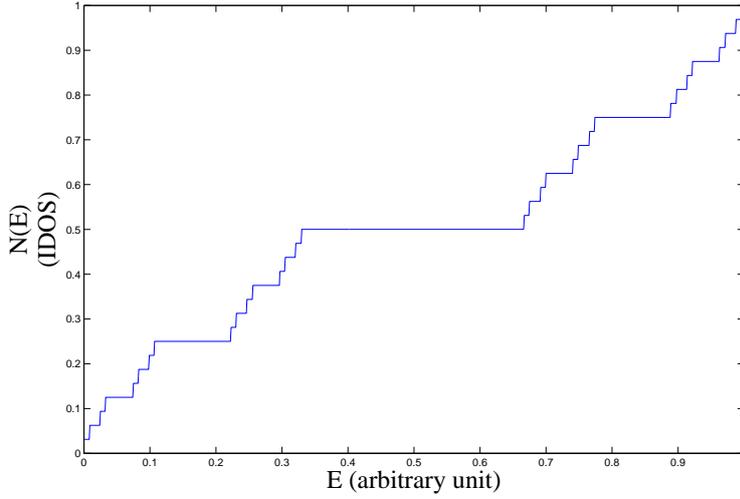
Figure 2: Integrated density of states (IDOS) in the case of a triadic Cantor set energy spectrum. The energies are expressed in arbitrary unit and the IDOS has been normalised.

$$
\int\limits_{K \times K} f(x,y)d\mu(x)d\mu(y) = \frac{1}{4} \int\limits_{K \times K} f\left(\frac{x}{3}, \frac{y}{3}\right) d\mu(x)d\mu(y)
$$

$$
+ \quad \frac{1}{4} \int\limits_{K \times K} f\left(\frac{x+2}{3}, \frac{y}{3}\right) d\mu(x)d\mu(y)
$$

$$
+ \quad \frac{1}{4} \int\limits_{K \times K} f\left(\frac{x}{3}, \frac{y+2}{3}\right) d\mu(x)d\mu(y)
$$

$$
+ \quad \frac{1}{4} \int\limits_{K \times K} f\left(\frac{x+2}{3}, \frac{y+2}{3}\right) d\mu(x)d\mu(y)
$$

Using (1), we find that the integrated density of states for this measure, $\mathcal{N}(\epsilon) = \int_K \theta(\epsilon - \epsilon')d\mu(\epsilon')$, verifies the scaling property :

$$
\mathcal{N}(\epsilon) = 2\mathcal{N}(\epsilon/3)
$$

Its graph is called a devil's staircase (see fig. (2)).

Note that the measure μ is a special case of a self-similar measures m, e.g. such that there exists a set of contractive similarities $\{\phi_j\}$ and probability weights $\{\pi_j\}$ such that for any continuous function f, one has :

$$
\int f(x)dm(x) = \sum_j \pi_j \int f(\phi_j(x))dm(x)
$$

Cantor sets correspond to the case of two linear similarities, with $\pi_1 = \pi_2 = \frac{1}{2}$:

$$
\int f(x)dm(x) = \frac{1}{2} \int f(a_1 x)dm(x) + \frac{1}{2} \int f(a_2 x + b)dm(x)
$$

The methods developed hereafter can easily be translated for any self-similar measure.

Let us now study the dynamics of the system described in the previous paragraph.

3.1 Time-averaged return probability

3.1.1 Analytical expression

There are several physical quantities which are useful to characterize the evolution of the system, such as the RMS displacement, the participation ratio or the return probability.

We will focus first on the time-averaged return probability function, as it is a very instructive example to understand how the scaling symmetry of the spectrum affects the dynamics of the system.

The time-averaged return probability, $C(t)$, is by definition the time average of the probability $p(t) = |\langle \psi(0)|\psi(t)\rangle|^2$ to find the system in its initial state after a time t :

$$C(t) = \frac{1}{t} \int_0^t |\langle \psi(0)|\psi(t')\rangle|^2 dt'$$

We could directly try to calculate $p(t)$ to study the evolution in time of the system ; however this quantity often exhibits fast local oscillations, which could hide the effects of the fractal feature. Its time average, on the other hand, yields interesting results.

We start with the spectral decomposition of $|\psi(t)\rangle$:

$$|\psi(t)\rangle = \int_{spectrum} g(\epsilon) e^{-i\epsilon t} |\phi(\epsilon)\rangle d\tilde{\mu}(\epsilon)$$

We impose that $|\psi(t)\rangle$ is normalized to unity :

$$\langle \psi(t)|\psi(t)\rangle = \int_{spectrum} |g(\epsilon)|^2 d\tilde{\mu}(\epsilon) = 1$$

We shall assume that $|g(\epsilon)|$ is non-zero and uniform on a bounded subset of the spectrum, and that this subset is triadic Cantor set. We therefore consider that $|g(\epsilon)|^2 d\tilde{\mu}(\epsilon)$ (the spectral measure of the initial state) is the measure $d\mu$ introduced in the previous paragraph.

Thus :

$$\begin{aligned} C(t) &= \frac{1}{t} \int_0^t |\langle \psi(0)|\psi(t')\rangle|^2 dt' \\ &= \frac{1}{t} \int_0^t |\int_K e^{-i\epsilon t'} d\mu(\epsilon)|^2 dt' \end{aligned}$$

A standard calculation then leads to :

$$C(t) = \int_{K \times K} \text{sinc}((\epsilon' - \epsilon)t) d\mu(\epsilon) d\mu(\epsilon')$$

The idea is now to transform this double integral into a one variable integral, and then to use Mellin transform and the scaling property (1) of $d\mu$.

Let us do the change of variables : $l = |\epsilon' - \epsilon|$, $0 \leq l \leq 1$, and let $dS(l, \mu)$ be the surface (in the sense of $d\mu$) of the 2 dimensional Cantor dust[2] contained in the two strips of infinitesimal width located at $\epsilon = \epsilon' + l$ and $\epsilon = \epsilon' - l$ (fig. 3).

Since $\text{sinc}((\epsilon' - \epsilon)t)$ can be considered constant on these strips, we obtain :

$$C(t) = \int_0^1 \text{sinc}(lt) dS(l, \mu) \tag{2}$$

We now have to determine $dS(l, \mu)$. For this we shall use Mellin transforms. The full calculation is given in the appendix. We find :

---

[2] obtained by iteration of the following process : start with a full square, divide it in 9 equal squares and keep only the four at the corners of the initial square ; see fig.(2)
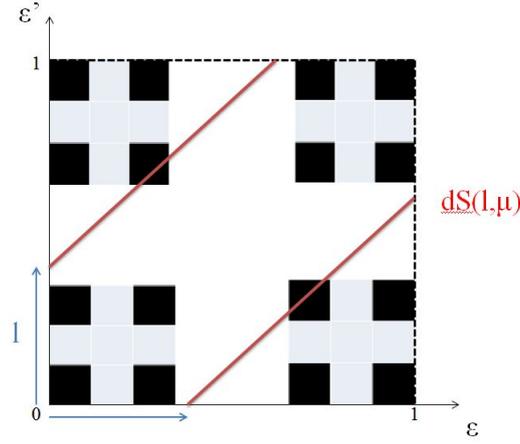
Figure 3: 2 dimensional Cantor dust (represented here at the second step of construction) ; the infinitesimal surface $dS(l, \mu)$ corresponds to the surface of the Cantor dust, in the sense of $d\mu$, contained in the two red strips.

$$\frac{dS(l,\mu)}{dl} = \sum_n \left[\frac{s - s_n}{1 - \frac{3^{1-s}}{2}} l^{-s} \gamma(s) \right]_{s=s_n}$$

$$= \frac{l^{d_K - 1}}{\ln(3)} \sum_n l^{\frac{2i\pi n}{\ln(3)}} \underbrace{\gamma \left(1 - d_K - \frac{2i\pi n}{\ln(3)} \right)}_{\gamma_n}$$

with $d_K = \frac{\ln(2)}{\ln(3)}$ and

$$\gamma_n = \int_{K \times K} |x - y + 2|^{-d_K - \frac{2i\pi n}{\ln(3)}} d\mu(x) d\mu(y)$$

Inserting this expression in (2), we get :

$$C(t) = \frac{1}{\ln(3)} \sum_{n \in \mathbb{Z}} \gamma_n \int_0^1 l^{d_K - 1} l^{2i\pi n / \ln(3)} \gamma_n \mathrm{sinc}(lt) dl$$

$$= \frac{t^{-d_K}}{\ln(3)} \sum_{n \in \mathbb{Z}} \gamma_n t^{-2i\pi n / \ln(3)} \int_0^t v^{d_K - 1 + 2i\pi n / \ln(3)} \mathrm{sinc}(v) dv$$

with the change of variable : $v = tl$. Since $\int_0^t v^{d + \frac{2i\pi n}{\ln(3)} - 1} \mathrm{sinc}(v) dv$ quickly converges to $\int_0^\infty v^{d_K + \frac{2i\pi n}{\ln(3)} - 1} \mathrm{sinc}(v) dv$, one can replace $\int_0^u$ by $\int_0^\infty$.

(More precisely : $|\int_0^u v^{d_K + \frac{2i\pi n}{\ln(3)} - 1} \mathrm{sinc}(v) dv - \int_0^\infty v^{d_K + \frac{2i\pi n}{\ln(3)} - 1} \mathrm{sinc}(v) dv| = O(u^{d_K - 1})$)

Using :

$$\int_0^\infty v^{d_{K_n} + \frac{2i\pi n}{\ln(3)} - 1} \mathrm{sinc}(v) dv$$

$$= \sin \left(\frac{\pi}{2} (d_{K,n} - 1) \right) \Gamma \left(d_{K,n} + \frac{2i\pi n}{\ln(3)} - 1 \right)$$

with Γ the Euler gamma function, and $d_{K,n} = d_K + \frac{2i\pi n}{\ln(3)}$ one finally finds

$$C(t) = \frac{t^{-d_K}}{\ln(3)} \sum_n \gamma_n t^{-\frac{2i\pi n}{\ln(3)}} a_n \left[1 + \mathcal{O}(t^{-1}) \right] \tag{3}$$

8

with $a_n = \sin\left(\frac{\pi}{2}(d_{K,n} - 1)\right)\Gamma(d_{K,n} - 1)$, and in the limit $t >> 1$ (see fig. (4), (5)):

$$C(t) = \frac{t^{-d_K}}{\ln(3)}\sum_n \gamma_n t^{-\frac{2i\pi n}{\ln(3)}}\sin\left(\frac{\pi}{2}(d_{K,n} - 1)\right)\Gamma(d_{K,n} - 1)$$
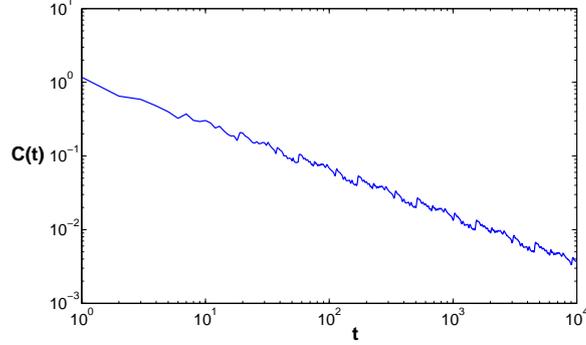

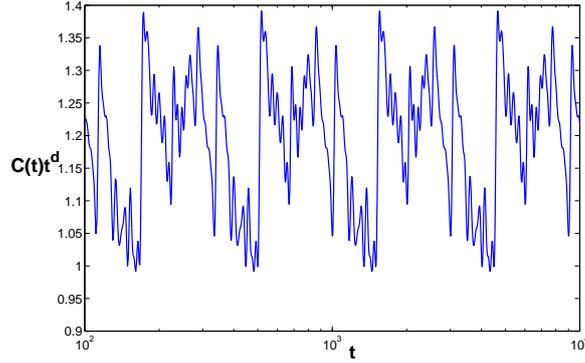Figure 4: Auto-correlation function in the case of a triadic Cantor set spectrum, in log-scale (log base 10).

Figure 5: Auto-correlation function multiplied by t^{d_K} in the case of a triadic Cantor set spectrum, in log-scale (log base 10). This function is log-periodic in t, of period $\ln(3)$.

We can prove that the coefficients in the expression (3) decay at least like $\frac{1}{n^{3/2-d}}$:

$$\left|\gamma_n \sin\left(\frac{\pi}{2}(d + \frac{2i\pi n}{\ln(3)} - 1)\right)\Gamma(d + \frac{2i\pi n}{\ln(3)} - 1)\right| = O\left(\frac{1}{n^{3/2-d}}\right)$$

Let us now discuss the expression of $C(t)$. We find that, asymptotically, $C(t)$ is of the form :
$C(t) = t^{-d_K}g(\ln t)$, with $d_K = \frac{\ln(2)}{\ln(3)}$ the fractal dimension of the triadic Cantor set K and

$$g(\ln t) = \sum_{n\in\mathbb{Z}}\gamma_n e^{-\frac{2i\pi n}{\ln(3)}\ln t}\sin\left(\frac{\pi}{2}(d_n - 1)\right)\Gamma(d_n - 1)$$

with $d_n = d + \frac{2i\pi n}{\ln(3)}$, a periodic function. The presence of the fractal dimension d_K in the exponent is consistent with previous work on the asymptotic behaviour of the time-averaged return probability for a Cantor spectrum : $C(t) \sim_{t\to\infty} t^{-d_k}$([5], [6]). Let us give an explanation for this specific exponent. Note that, asymptotically, $C(t)$ satisfies the functional equation :
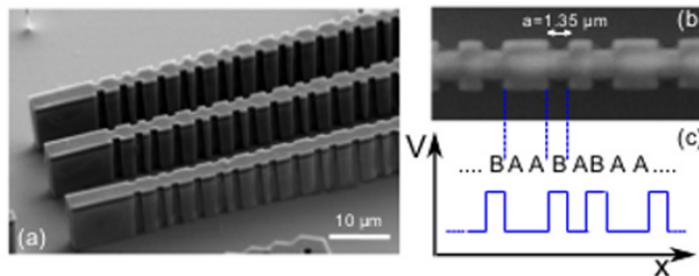
$$C(t) = \frac{1}{2}C(t/3)$$

9

Figure 6: (a) Photo of 3 cavities modulated according to the Fibonacci sequence. (b) Zoom on a cavity, showing the shape of the letters A and B. (c) Schematic representation of the potential corresponding to the shape of the cavity, laterally modulated. Source : [1]

which, according to the previous section, leads naturally to having $C(t)$ of the form :

$$C(t) = t^{-d_K} g(\ln t)$$

This means that $C(t)$ is a scaling function, with the scaling numbers of the Cantor set. The asymptotic behaviour of $C(t)$ can be intuited by the following observation : using the scaling property of the measure, we find that :

$$C(t) = \frac{1}{2}C(t/3) + \frac{1}{2}\iint_{K \times K} \text{sinc}(\frac{x - x' + 2}{3}t)d\mu(x)d\mu(x')$$

When $t \to \infty$, the second term of the sum on the right tends to zero, since for all x, x' in K, $1 < x - x' + 2 < 3$. Thus, $C(t)$ is asymptotically a scaling function :

$$C(t) \sim_{t \to \infty} \frac{1}{2}C(t/3)$$

We could have qualitatively predicted this by observing that $C(t) = \int_{K \times K} \text{sinc}((\epsilon' - \epsilon)t)d\mu(\epsilon)d\mu(\epsilon')$ is the wavelet transform of the spectrum, acting like a magnifying glass ; as t goes to infinity, the surface of integration is narrowed due to the sinc function, and decreases like $t^{-d_k}\mathcal{F}(\ln t)$, as we saw by calculating the area variation $dS(l, \mu)$. Thus, we expect to observe this typical behaviour in other dynamical quantities if they can be expressed as integrals over the spectrum ; in particular, this should be the case if we look at their time-average.

3.1.2 Experiment : Fibonacci cavity

Before discussing other quantities, let us highlight the similarity between the theoretical graph of $C(t)$ for a triadic Cantor set spectrum (fig. (4), (5)) and the numerical results obtained with the Fibonacci cavity (more details are available in [1]) fig. (6).

In this experiment, cavity polaritons are confined in wire cavities, consisting of $\lambda/2$ layers, using Bragg mirrors for the confinement in the vertical direction. The lateral dimension of the $200\mu m$ long wires are modulated quasi-periodically : the modulation consists in two wire sections (letters) A and B, of equal length but different width ; these letters are arranged in a finite sequence, S_j, obtained recursively using the following Fibonacci like algorithm : $S_{j>2} = [S_{j-1}S_{j-2}]$ and $S_1 = B$, $S_2 = A$ where $[S_{j-1}S_{j-2}]$ is the concatenation of the sequences S_{j-1} and S_{j-2}. The sequence S_∞ becomes rigorously quasi-periodic as j tends to infinity. We used a finite sized cavity, however, we observed the features of the fractal spectrum predicted by the theory : namely, gaps densely distributed and an integrated density of states $\mathcal{N}(\epsilon)$ well described by a scaling form of the type $\mathcal{N}(\epsilon) = \epsilon^{\ln a / \ln b}\mathcal{F}(\frac{\ln \epsilon}{\ln b})$ and which is given by the gap labelling theorem [8]. The photon modes are described by a 2D scalar wave equation with vanishing boundary conditions on the boundary of the wire. This 2D problem is then reduced to a 1D Schroedinger equation with an effective quasi-periodic potential, translating the geometry of the cavity. The equation was then solved numerically (using the transfer matrix formalism) and some useful quantities were plotted : the
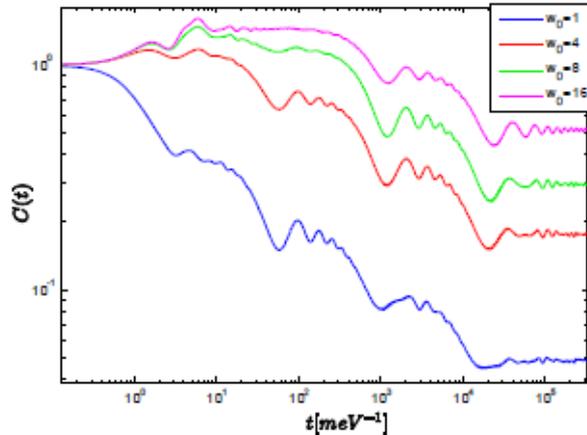
Figure 7: Auto-correlation function of the wave paquet in the Fibonacci cavity ; numerical results for an initial gaussian wave paquet : $\psi(x, t = 0) \sim e^{-2(x-x_0)^2/w_0^2}$. The graphs correspond to different values of w_0, with identical x_0.

IDOS, the participation ration, the RMS displacement and the time-averaged return probability. The latter is given fig. (7) ; we found that the return probability has a log-periodic structure, which is consistent with the theoretical results.

We also found that the participation ratio displays a log-periodic feature.

3.1.3 Generalization and discussion of the method used to derive $C(t)$

Let us now discuss the method used in a more general way, to highlight the connection between the presence of a scaling symmetry in a physical system and the typical form of certain quantities. We see from the calculation that the scaling property of the spectrum leads naturally to a specific behaviour of some physical quantities defined as integrals over the spectrum - power law modulated by log-periodic oscillations.

In the case of a fractal F described by a measure μ such that :

$$\int_F f(x)d\mu(x) = \sum_{n \in \mathbb{N}} \frac{1}{b_n} f(a_n x)d\mu(x)$$

for some $a_n \in \mathbb{R}$, $b_n \in \mathbb{R}*$, then any function $\Psi(t)$ defined by an integral : $\Psi(t) = \int_F h(x,t)d\mu(x)$ will satisfy :

$$\Psi(t) = \sum_{n \in \mathbb{N}} \frac{1}{b_n} \int_F h(a_n x, t)d\mu(x)$$

If furthermore $h(x,t)$ can be expressed as a function of $x^\alpha t^\beta$, $\alpha, \beta \in \mathbb{C}$, $\beta \neq 0$: $h(x,t) = \psi(x^\alpha t^\beta)$, then :

$$\begin{aligned}
\Psi(t) &= \sum_{n \in \mathbb{N}} \frac{1}{b_n} \int_F \psi(a_n x^\alpha t^\beta)d\mu(x) \\
&= \sum_{n \in \mathbb{N}} \frac{1}{b_n} \int_F h(x, a_n^{1/\beta} t)d\mu(x) \\
&= \sum_{n \in \mathbb{N}} \frac{1}{b_n} \Psi(a_n^{1/\beta} t) \\
&= \frac{1}{b_j} \Psi(a_j^{1/\beta} t) + \Phi(t)
\end{aligned}$$

with $\Phi(t) = \sum_{n \in \mathbb{N} - j} \frac{1}{b_n} \Psi(a_n^{1/\beta} t)$. Using the Mellin transform, under certain conditions (mainly, if the Mellin transforms of $\Phi(t)$ and $\Psi(t)$ exist and have overlapping domains of definition, and if
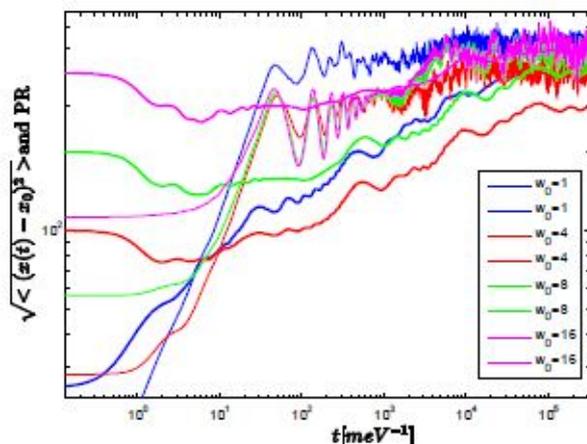
11

Figure 8: Participation ratio and RMS for the wave paquet in the Fibonacci cavity ; numerical results for an initial gaussian wave paquet : $\psi(x, t = 0) \sim e^{-2(x-x_0)^2/w_0^2}$. The graphs correspond to different values of w_0, with identical x_0.

the Mellin transform of $\Phi(t)$ has no poles), then $\Psi(t)$ will be of the form :

$$\Psi(t) = t^{\ln(b_j)/\ln(a_j^{1/\beta})} G\left(\frac{\ln t}{\ln a_j^{1/\beta}}\right)$$

with G 1-periodic.

More generally, this also occurs whenever we can rearrange the integral in order to have : $\int_F h(\alpha x, t) d\mu(x) \propto \int_F h(x, \beta t) d\mu(x)$.

Thus, we see in the case of quantum dynamics that, since the energy ϵ and the time t are conjugate variables (through the spectral decomposition), it is likely that many time dependant quantities have a log-periodic component. This is well verified for $C(t)$. Furthermore, we pointed out that time-averaging is equivalent to taking the wavelet transform of the spectrum, which we have shown to display a characteristic behaviour. Therefore, it is expected that other time-averaged dynamical quantities would naturally display the typical log-periodic structure. In fact, the time-average of the amplitude of the wave function at some point x in space, $\langle |\psi(x, t)|^2 \rangle = \frac{1}{t} \int_0^t |\psi(x, t')|^2 dt'$, is given by :

$$\langle |\psi(x, t)|^2 \rangle = \iint_K g(\epsilon')^* g(\epsilon) \phi_{\epsilon'}(x)^* \phi_{\epsilon}(x) \mathrm{sinc}((\epsilon - \epsilon')t) d\mu d\mu$$

The qualitative argument saying that, since the surface of integration decreases like $t^{-d_k} \mathcal{F}(\ln t)$ as $t \to \infty$ (due to the *sinc*), we expect to have a similar time-dependence for the global quantity. Since any dynamical quantity can be expressed using the wave function, this implies that this typical behaviour should be common to many quantities. However, more information about the eigenfunctions is usually required to study rigorously the dynamics of the system. We shall illustrate this by discussing now two other quantities which carry the fingerprint of the scaling symmetry of the spectrum : the root-mean displacement (RMS) and the participation ratio.

3.2 Other relevant quantities : participation ration, root-mean displacement

The time-averaged participation ratio is usually studied to get information on the dynamics of a quantum system. This quantity was studied numerically for the Fibonacci cavity (fig. (8)) and the results support the idea of a log-periodic feature.

By definition, the participation ratio is :

$$P_\psi = \frac{1}{\int_{espace} |\langle x | \psi \rangle|^4 dx}$$

12

It reflects the localization in space of the wave function $\psi(x, t)$: if the state is localized, then $P_\psi \simeq 0$; if it is extended, then $P_\psi \simeq 1$ [7]. Taking its time-average, to have a time-dependent quantity, we define :

$$P_\psi(t) = \frac{1}{t} \int_0^t \frac{dt'}{\int_{espace} |\langle x|\psi(t')\rangle|^4 dx}$$

The RMS displacement is commonly studied both in quantum dynamics - spreading of the wave packet - and in diffusive processes.

$$\Delta x = \sqrt{\langle (x(t) - x_0)^2 \rangle} = \sqrt{\int_{space} (x(t) - x_0)^2 |\psi(t,x)|^2 dx}$$

Neither of these quantities are pure spectral quantities, as opposed to $C(t)$ which we managed to express only in terms of the eigenvalues of the system. Here, more information about the eigenfunctions ϕ_ϵ is required to go further. To do so, we focused on the tight-binding model.

3.3   Tight-binding-model

In order to have a better understanding of the dynamics of our system, we consider the case of the tight-binding model.

We consider an infinite 1D lattice, with sites k labelled from 0 to infinity. We define a potential V on this system such that the discrete Schrodinger operator : $H = -\Delta + V$, which acts on $l_2(\mathbb{Z})$, has a triadic Cantor set spectrum. The eigenfunctions of H verify :

$$H\phi_\epsilon(k) = \epsilon\phi_\epsilon(k)$$

3.3.1   Identification of a simple set of functions describing the dynamics of the system

In the tight-binding model, the above equation becomes :

$$-\phi_\epsilon(k+1) - \phi_\epsilon(k-1) + 2\phi_\epsilon(k) + V(k)\phi_\epsilon(k) = \epsilon\phi_\epsilon(k)$$

or, using transfer matrices :

$$\begin{pmatrix} \phi_\epsilon(k) \\ \phi_E(k-1) \end{pmatrix} = \begin{pmatrix} 2 + V_k - \epsilon & -1 \\ 1 & 0 \end{pmatrix} \begin{pmatrix} \phi_\epsilon(k) \\ \phi_\epsilon(k-1) \end{pmatrix}$$

Imposing $\phi_\epsilon(0) = 0$, we find that the eigenfunctions $\{\phi_\epsilon\}_{\epsilon \in K}$, evaluated on the sites k, can be seen as polynomials in ϵ :

$$\phi_\epsilon(k) = \phi_\epsilon(1)p_k(\epsilon) \tag{4}$$

with

$$\begin{pmatrix} p_k(\epsilon) & q_k(\epsilon) \\ p_{k-1}(\epsilon) & q_{k-1}(\epsilon) \end{pmatrix} = \prod_{j=k}^{1} \begin{pmatrix} 2 + V_j - \epsilon & -1 \\ 1 & 0 \end{pmatrix}$$

The polynomials $\{p_k(\epsilon)\}$ verify the recurrence relation :

$$p_{k+1}(\epsilon) = (2 + V_{k+1} - \epsilon)p_k(\epsilon) - p_{k-1}(\epsilon)$$

with initial conditions : $\begin{cases} p_1(\epsilon) = 2 + V_1 - \epsilon \\ p_0(\epsilon) = 1 \end{cases}$ We are interested of the evolution of a wave packet, described by the normalized wave function $\psi(t)$, evolving according to Schrodinger's equation :

$$i\frac{d\psi(t)}{dt} = H\psi(t)$$

The wave function is initially localized at the site 1 : $\langle k|\psi(t=0)\rangle = \delta(k-1)$. At time t, the system is in the state : $|\psi(t)\rangle = e^{-iHt}|\psi(0)\rangle$, and the value of the wave function at site k is given by :

$$|\psi(k,t)| = \int_K \phi_\epsilon(1)^* \phi_\epsilon(k) e^{-i\epsilon t} d\mu$$

13

Using (4), we obtain :

$$\psi(k,t) = \int_K \phi_\epsilon(1)^* \phi_\epsilon(k) e^{-i\epsilon t} d\mu$$

$$= \int_K |\phi_\epsilon(1)|^2 p_k(\epsilon) e^{-i\epsilon t} d\mu$$

$$= \sum_{j_k \leq k} c_{j_k} \int_K \epsilon^{j_k} e^{-i\epsilon t} d\mu$$

with $p_k(x) = \sum_{0 \leq j_k \leq k} c_{j_k} x^{j_k}$ and where we defined, as in the previous section, the local measure associated to the state $|\psi\rangle$: $d\mu = |\phi_\epsilon(1)|^2 d\mu$.

Thus, the dynamical behaviour of the system depends essentially on the functions :

$$h_k(t) = \int_K e^{-i\epsilon t} \epsilon^k d\mu(\epsilon)$$

aka the Fourier transforms on K of the moments x^k.

Expending the exponential in $h_k(t)$, we obtain :

$$h_k(t) = \sum_{n \leq 0} \frac{(-it)^n}{n!} \mu_{n+k}$$

with $\mu_n = \int_K x^n d\mu$.

The fingerprint of the scaling symmetry of the spectrum is carried by the $\mu_n = \int_K x^n d\mu$. It can be shown that, for $n \to \infty$ (see [10])

$$\mu_n = n^{-\ln 2/\ln 3} F(\ln n / \ln 3)(1 + O(\frac{1}{n}))$$

where F is a log-periodic function of period 1.

The $h_k(t)$ do not verify a scaling property (of the form $f(x) = bf(ax)$) ; however, there is a structure and there are some scaling invariance, the details of which are given in the appendix. The main results are that :
- the zeroes of $h_k(t)$ are those of $h_{k-1}(t/3)$, as illustrated in fig. (16)
- at local maxima, the amplitude of the functions $h_k(t)$ decreases with k.

We wish now to examine how this structure translates in terms of physical dynamical quantities. Although the $h_k(t)$ are not scaling functions, the relations between the zeroes of h_k and the behaviour at the local maxima justify the numerical observation that, approximately
$h_k(t) \propto h_{k-1}(t/3)$.

3.3.2 RMS without time-averaging

This almost re-scaling relation translates to the RMS :

$$\Delta x(t) = \sum_{k=1}^{\infty} k^2 |\psi(k,t)|^2$$

$$= \sum_{k=1}^{\infty} k^2 | \sum_{j_k \leq k} c_{j_k} \int_K \epsilon^{j_k} e^{-i\epsilon t} d\mu |^2$$

$$= \sum_{k=1}^{\infty} k^2 | \sum_{j_k \leq k} c_{j_k} h_{j_k}(t) |^2$$

$$\propto \sum_{k=1}^{\infty} k^2 | \sum_{j_k \leq k} c_{j_k} h_{j_k - 1}(t/3) |^2$$

$$\propto \Delta x(t/3)$$

14

Note that there is not a perfect proportionality between $\Delta x(t)$ and $\Delta x(t/3)$; there is an approximate proportionality relation, due to the structure of the functions $h_k(t)$ which is preserved under $t \to t/3$. According to the mathematical prerequisites, if $\Delta x(t) \propto \Delta x(t/3)$, then $\Delta x(t)$ is a scaling function and is therefore of the form : $\Delta x(t) = t^\alpha G(\ln t)$, with $\alpha \in \mathbb{R}$ and G periodic. Even with an approximate proportionality relation, we expect nevertheless to observe the log-periodic structure. We will verify this assumption numerically in a few paragraphs.

3.3.3 Time-averaging

We discuss here the influence of time-averaging. First, we study $\frac{1}{t}|\psi(k,t')|^2 dt'$, which narrows down to the study of the quantities :

$$\frac{1}{t}\int_0^t h_k^*(t')h_l(t')dt'$$

Since $|\psi(k,t)|^2$ is real, we need only to consider the real part of $\frac{1}{t}\int_0^t h_k^*(t')h_l(t')dt'$, which we note $f_{k,l}(t)$. A standard calculation leads to :

$$f_{k,l}(t) = \Re\left(\frac{1}{t}\int_0^t h_k^*(t')h_l(t')dt'\right)$$
$$= \iint_{K \times K} x^k x'^l \text{sinc}((x'-x)t)d\mu(x)d\mu(x')$$

Note that $f_{0,0}(t)$ is the time-averaged return probability $C(t) = \frac{1}{t}\int_0^t |\langle\psi(0)|\psi(t')\rangle|^2 dt'$, which we derived earlier.

For the calculation of $C(t)$, we used the change of variable $l = |x - x'|$ and reduced the problem to calculating the area $dS(l, \mu)$. The log-periodic behaviour comes from the expression of $dS(l, \mu)$.

If we make the approximation that : $sinc(xt) = 1$ for $|xt| < \pi$ and $sinc(xt) = 0$ elsewhere, we get the following approximate expression for $C(t)$:

$$C(t) = \int_{l=0}^{\pi/t} dS(l, \mu) = t^{-\ln 2/\ln 3} \sum_n d_n t^{-2i\pi n/\ln 3}$$

which accounts for the typical asymptotic behaviour, although the coefficients d_n are a little bit different from the coefficients in the exact expression.

If we apply the same reasoning for

$$f_{k,l}(t) = \iint x^k x'^l sinc((x'-x)t)d\mu(x)d\mu(x')$$

we find :

$$f_{k,l}(t) \approx \iint_{|x-x'|<\frac{\pi}{t}} x^k x'^l d\mu(x)d\mu(x')$$

As t goes to infinity, the area on which we integrate gets smaller, and decreases like $t^{-\ln 2/\ln 3}G(\ln t/\ln 3)$, with G a periodic function. Therefore, the integral $f_{k,l}(t)$ should display a similar behaviour ; even though we did not derive a full analytical expression yet, a numerical study confirms this assumption (see fig. (9)) : $f_{k,l}(t)$ is a power-law $t^{-\ln 2/\ln 3}$ modulated by log-periodic oscillations.

This implies that the wave function has the following asymptotic behaviour : $\frac{1}{t}\int_0^t |\psi(k,t')|^2 dt' \sim t^{-\ln 2/\ln 3}$; from here we may deduce, adapting the argument of Guarneri in [11], that the time-averaged RMS has the asymptotic lower bound :

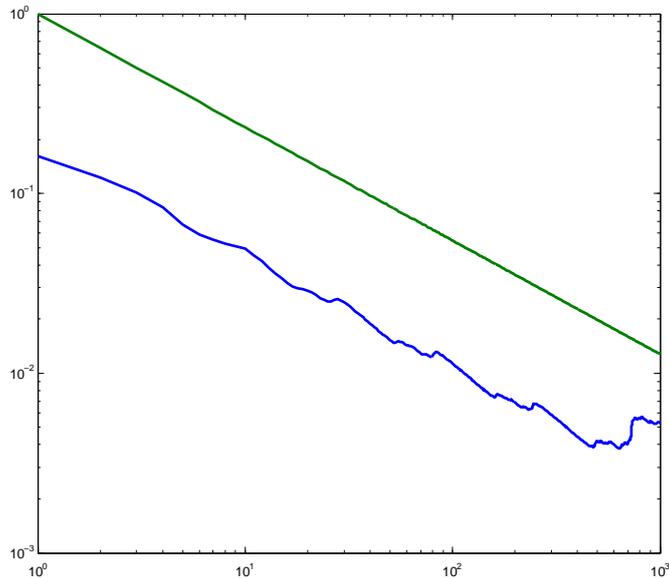$$\sqrt{\frac{1}{t}\int_0^t \Delta x^2(t')dt'} \geq \frac{t^{\frac{\ln 2}{\ln 3}}}{\ln t}$$

15

Figure 9: Loglog scale graphs of $f_{1,2}(t)$ (green) and $t^{-\ln 2/\ln 3}$ (blue)

3.3.4 Numerical study

In order to verify the theoretical results of the above question, we study numerically a quantum system in the tight-binding model. We consider first the case of a Fibonacci potential, to verify the formula :

$$\phi_\epsilon(k) = \phi_\epsilon(1)p_k(\epsilon)$$

and to compare the graphs of the numerical RMS in our model with the literature (the Fibonacci potential having been widely studied in the past decades, see [12], [13] and references therein). The Fibonacci potential is constructed recursively, using the Fibonacci sequence, as for the Fibonacci cavity : we label the sites of the system using letters A and B according to the algorithm described for the experiment with polaritons, and define the potential : $\begin{cases} V(k) = 0.6 \text{ if site } k \equiv A \\ V(k) = -0.6 \text{ if site } k \equiv B \end{cases}$

The associated energy spectrum is given fig. (10).

We will then study a quantum system with an associated triadic Cantor set spectrum.

For the numerics, we consider a finite system of 233 sites for the Fibonacci potential, and 256 sites for the Cantor set. The Hamiltonian is modelized by a tridiagonal matrix.

We find that the formula $\phi_\epsilon(k) = \phi_\epsilon(1)p_k(\epsilon)$ is very well verified for both systems.

Let us now study the dynamics. In both cases the wave packet is initially localized on the first site $k = 1$.
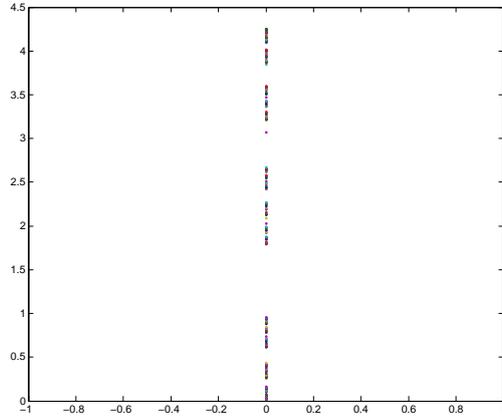
16

Figure 10: Energy spectrum (arbitrary units) for the Fibonacci potential.

The graph of the RMS for the Fibonacci potential has the expected log-periodic behaviour, which is consistent with previous results ([13]) and with our theoretical prediction (since the associated energy spectrum for a Fibonacci potential is Cantor-like, the arguments of the above paragraphs can be adapted).

We find for the triadic Cantor spectrum that $\Delta x(t)$ has a log-periodic structure : it displays oscillations, which have a log-periodic envelope of period $\log 3$; inside the envelope, the period of the oscillations increases with time, which is consistent with the behaviour of $h_k(t)$ under the transformation $t \to t/3$. We find numerically that : $\Delta x(t) \approx \frac{3}{2}\Delta x(t/3)$ (see fig. (11)), which suggests that $\Delta x(t)$ also has a power-law component. The time-averaged quantity has the expected log-periodic structure, and also verifies the lower bound (see fig. (12))

$$\sqrt{\frac{1}{t}\int_0^t \Delta x^2(t')dt'} \geq t^{\frac{\ln 2}{\ln 3}}/\ln t$$

The instantaneous participation ratio does not seem to have a log-periodic structure, but its time-average displays a log-periodicity (see fig. (13)).
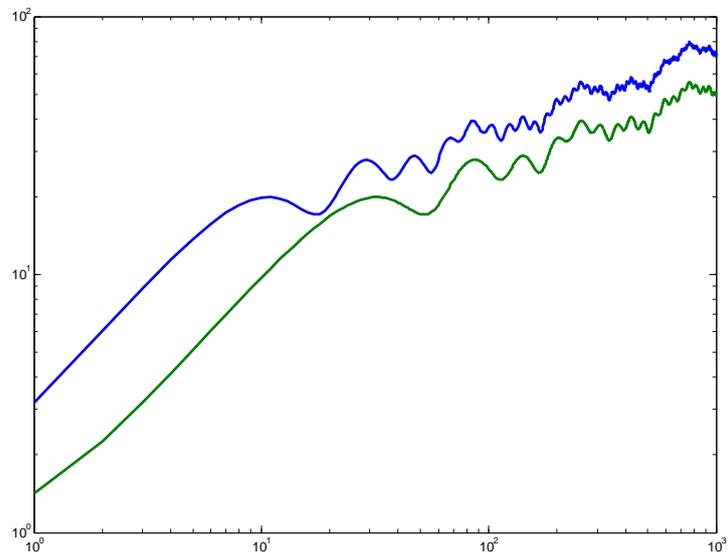
17

Figure 11: RMS for a triadic Cantor spectrum as a function of time, in loglog scale ; blue : $\Delta x(t)$, green : $\Delta x(t/3)$.
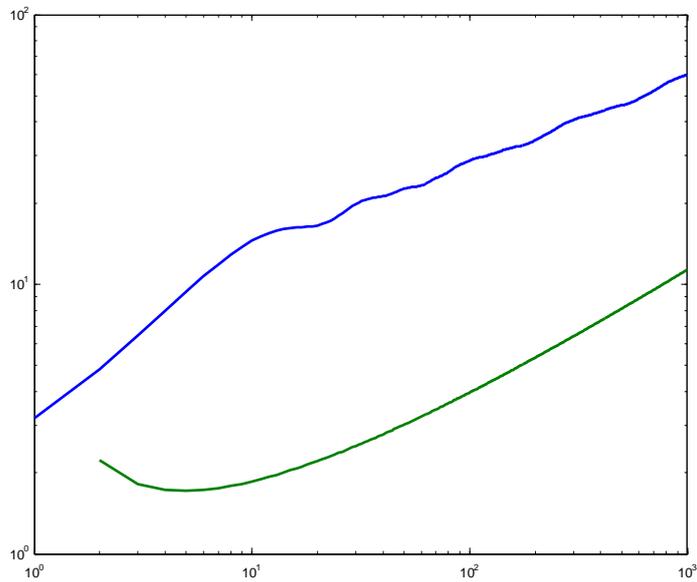
Figure 12: Loglog scale graphs of $\sqrt{\frac{1}{t}\int_0^t \Delta x^2(t')dt'}$ (blue) and $t^{\frac{\ln 2}{\ln 3}}/\ln t$ (green)
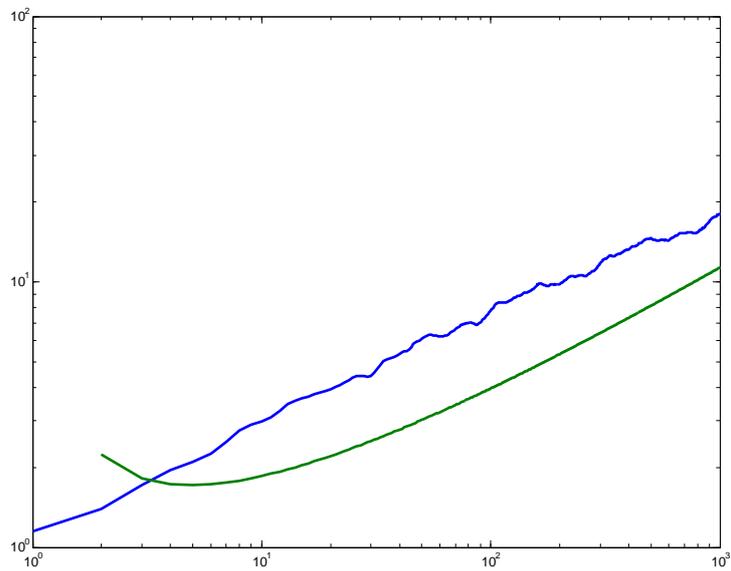
19

Figure 13: Time-averaged participation for a triadic Cantor spectrum (blue) ; lower-bound $t^{-\ln 2/\ln 3}/\ln t$ (green) ; loglog scale.

3.4 Thouless coefficient

Here we mention briefly another quantity, commonly studied to characterize the dynamics of a wave packet : the Thouless coefficient (see [8], [9]), defined by :

$$\gamma(E) = \int_{spectrum} \ln|y - E| d\mu(y)$$

for $E \in$ spectrum In the case of a Cantor spectrum, we find that $\gamma(E)$ displays a self-similarity, which translates the presence of a self-similar fractal spectrum (see fig. (14)), and verifies the following functional equation :

$$\gamma(x) = -\ln 3 + \frac{1}{2}\gamma(3x) + \frac{1}{2}\gamma(3x + 2)$$
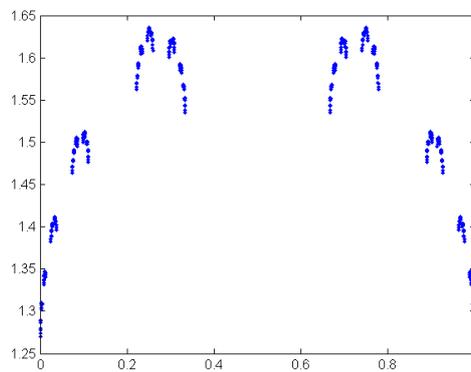

Figure 14: Thouless coefficient for a triadic Cantor spectrum.

4   Conclusion and perspectives

We identified the fingerprint of a self-similar spectrum in the dynamics of a quantum system. Due to the scaling symmetry of the spectrum, some physical dynamical quantities are scaling functions, meaning they are of the form : $f(t) = t^\alpha G(\ln t)$ with $\alpha \in \mathbb{R}$ and G periodic. Thus, the scaling symmetry of the spectrum is visible in dynamical quantities through the presence of a power-law modulated by log-periodic periodic oscillations. Using the Mellin transform, we derived the analytical expression of the time-averaged return probability $C(t)$, which is universal for any system with a Cantor spectrum. We found that $C(t)$ is asymptotically a scaling function, of the form :

$$C(t) =_{t \to \infty} \left(\frac{t}{\tau} \right)^{-d_K} g(\ln(t/\tau))$$

where $d_K = \frac{\ln(2)}{\ln(3)}$ is the fractal dimension of the triadic Cantor set, τ a time scale a g a periodic function which we calculate exactly. Note that, therefore, one can deduce the spectral dimension of a given system by studying the time-averaged return probability. This result is supported by numerical results obtained recently for polaritons in a Fibonacci potential.

We gave a more thorough analysis in the case of the tight-binding model, in which case the dynamics of the system depend essentially on the Fourier transform on a Cantor set of monomes x^k, namely : $h_k(t) = \int_K e^{-ixt} x^k d\mu$, $k \in \mathbb{Z}$, which carry the fingerprint of the spectral fractal feature.

Further perspectives will be to apply the methods developed to the study of superradiance. In fact, we used a similar method to derive the decay probability of a two level atom coupled to a fractal spectrum ([14]). We showed that, in this case, Fermi's golden rule does not hold, and that the decay probability of the atom from an energy level E_i to an energy $E_f \pm \Delta E$ is of the form (5). Now, since the techniques used to study the dynamics of a wave packet for a fractal spectrum rely essentially on the scaling symmetry of the spectrum, we wish to adapt them to study analytically the resolvent of the Hamiltonian in the case of spontaneous emission and superradiance, which will give precious informations on the evolution of the system.

5 Appendix

5.1 Log-periodicity of the functions verifying $f(x) = \frac{1}{b}f(ax)$

We show here that a function f displays verifying the functional equation :

$$f(x) = \frac{1}{b}f(ax)$$

for some real numbers (a, b), $b \neq 0$ is of the form

$$f(x) = x^{\ln(b)/\ln(a)} g\left(\frac{\ln(x)}{\ln(a)}\right)$$

with g a periodic function of period 1 : $g(x+1) = g(x)$.

  - if $b = 1$, we may define h such that : $h(x) = f(e^{x \ln(a)})$ (change of variable), and we verify that :

$$h(x+1) = f(e^{(x+1)\ln(a)}) = f(e^x a) = f(e^x) = h(x)$$

f is therefore of the form : $f(x) = h\left(\frac{\ln x}{\ln a}\right)$ with h 1-periodic.

  - if $b \neq 1$, we go back to the previous case by noticing that $k(x) = f(x)x^{-\ln(b)/\ln(a)}$ verifies $k(ax) = k(x)$.

This completes the proof.

5.2 Scaling property of the measure $d\mu$

Let f be an integrable function on $[0, 1]$, either real or complex.

We show here that :

$$\int_K f(x)d\mu(x) = \frac{1}{2}\int_K f\left(\frac{x}{3}\right)d\mu(x) + \frac{1}{2}\int_K f\left(\frac{x+2}{3}\right)d\mu(x)$$

By the definition of $d\mu$:

$$\int_K f(x)d\mu(x) = \lim_{n\to\infty} \underbrace{\left(\frac{2}{3}\right)^n \sum_{a_{j_n}\in P_n}\int_{a_{j_n}}^{a_{j_n}+3^{-n}} f(x)dx}_{I_n(f(x))}$$

with P_n the set of the left edges of the remaining segments after n steps in the construction of the triadic Cantor set K. It is straightforward to verify that the sequence $(P_n)_n$ satisfies the following recurrence relation : $P_n = \frac{1}{3}P_{n-1} \cup \{\frac{2}{3} + \frac{1}{3}P_{n-1}\}$. Thus :

$$I_n(f(x)) = \left(\frac{2}{3}\right)^n \sum_{a_{j_n}\in P_n}\int_{a_{j_n}}^{a_{j_n}+3^{-n}} f(x)dx$$

$$= \left(\frac{2}{3}\right)^n \left[\sum_{a_{j_{n-1}}\in P_{n-1}}\int_{a_{j_{n-1}}/3}^{a_{j_{n-1}}/3+3^{-n}} f(x)dx + \sum_{a_{j_{n-1}}\in P_{n-1}}\int_{\frac{2}{3}+a_{j_{n-1}}/3}^{\frac{2}{3}+a_{j_{n-1}}/3+3^{-n}} f(x)dx\right]$$

changement de variable : $u = 3x$, $v = 3x - 2$

$$= \left(\frac{2}{3}\right)^n \left[\sum_{a_{j_{n-1}}\in P_{n-1}}\int_{a_{j_{n-1}}}^{a_{j_{n-1}}+3^{-n+1}} f\left(\frac{u}{3}\right)\frac{du}{3} + \sum_{a_{j_{n-1}}\in P_{n-1}}\int_{a_{j_{n-1}}}^{a_{j_{n-1}}+3^{-n+1}} f\left(\frac{v+2}{3}\right)\frac{dv}{3}\right]$$

$$= \frac{3}{2}\frac{1}{3}\left[I_{n-1}\left(f\left(\frac{u}{3}\right)\right) + I_{n-1}\left(f\left(\frac{2+v}{3}\right)\right)\right]$$

But : $\lim_{n\to\infty} I_{n-1}\left(f\left(\frac{u}{3}\right)\right) = \int_K f\left(\frac{u}{3}\right) d\mu(u)$ and $\lim_{n\to\infty} I_{n-1}\left(f\left(\frac{2+v}{3}\right)\right) = \int_K f\left(\frac{2+v}{3}\right) d\mu(u)$, therefore, finally :

$$\int_K f(x)d\mu(x) = \frac{1}{2}\int_K f\left(\frac{x}{3}\right) d\mu(x) + \frac{1}{2}\int_K f\left(\frac{x+2}{3}\right) d\mu(x)$$

which is what we wanted to prove.

5.3 Derivation of $dS(l, \mu)$

We calculate here the infinitesimal area $dS(l, \mu)$ introduced in section 1. The idea is to take the Mellin transform of $dS(l, \mu)$, study its poles in the complex plan by using property (1), and find $dS(l, \mu)$ by applying the inverse Mellin transform and the residue formula.

Let : $M_{dS}(s) = \int_0^1 l^{s-1} dS(l, \mu) = \int_0^1 l^{s-1}\frac{dS(l,\mu)}{dl} dl$ be the Mellin transform of $dS(l, \mu)$, which is sometimes referred to in the literature as the energy integral [15] (note that we wrote $\int_0^1$ and not $\int_0^\infty$: $dS(l, \mu)$ is defined on $[0, 1]$, but can be extended on $[0, \infty[$ if we define it as equal to 0 outside $[0, 1]$). Now, using the definition of $dS(l, \mu)$ and the property (1) :

$$
\begin{aligned}
M_{dS}(s) &= \int_0^1 l^{s-1} dS(l, \mu) \\
&= \int_{K\times K} |x - y|^{s-1} d\mu(x)d\mu(y) \\
&= \frac{1}{4}\int_{K\times K}\left(|\frac{x}{3} - \frac{y}{3}|^{s-1} + |\frac{x+2}{3} - \frac{y+2}{3}|^{s-1}\right) d\mu(x)d\mu(y) \\
&\quad + \frac{1}{4}\int_{K\times K}\left(|\frac{x}{3} - \frac{y+2}{3}|^{s-1} + |\frac{x+2}{3} - \frac{y}{3}|^{s-1}\right) d\mu(x)d\mu(y) \\
&= \underbrace{\frac{3^{1-s}}{2}\int_{K\times K}|x - y|^{s-1} d\mu(x)d\mu(y)}_{M_{dS}(s)} \\
&\quad + \underbrace{\frac{3^{1-s}}{2}\int_{K\times K}|x - y + 2|^{s-1} d\mu(x)d\mu(y)}_{\gamma(s)}
\end{aligned}
$$

Thus :

$$M_{dS}(s) = \frac{\gamma(s)}{1 - 3^{1-s}/2}$$

with $\gamma(s) = \frac{3^{1-s}}{2}\int_{K\times K}|x - y + 2|^{s-1} d\mu(x)d\mu(y)$.

The inverse Mellin transform then gives $\frac{dS(l,\mu)}{dl}$:

$$
\begin{aligned}
\frac{dS(l, \mu)}{dl} &= \frac{1}{2i\pi}\int_{\gamma-i\infty}^{\gamma+i\infty} M_{dS}(s)l^{-s} ds \\
&= \frac{1}{2i\pi}\int_{\gamma-i\infty}^{\gamma+i\infty}\frac{\gamma(s)}{1 - \frac{3^{1-s}}{2}} l^{-s} ds
\end{aligned}
$$

It is important to note that $\gamma(s)$ has no poles. It is clear from its definition :

$$\gamma(s) = \frac{3^{1-s}}{2}\int_{K\times K}|x - y + 2|^{s-1} d\mu(x)d\mu(y)$$

Since for all $x, y \in [0, 1]$, the inequality $1 \leq 2 - x + y \leq 3$ holds, $|x - y + 2|^{s-1}$ is well defined and bounded on $K \times K$ for any $s \in \mathbb{C}$, and thus $\gamma(s)$ is well defined and has no poles. The only poles of $\frac{\gamma(s)}{1 - \frac{3^{1-s}}{2}} l^{-s}$ are the $\{s_n\}_{n\in\mathbb{Z}}$ such that : $1 - s_n = \frac{\ln(2)}{\ln(3)} + \frac{2i\pi n}{\ln(3)}$. We now apply the residue theorem :
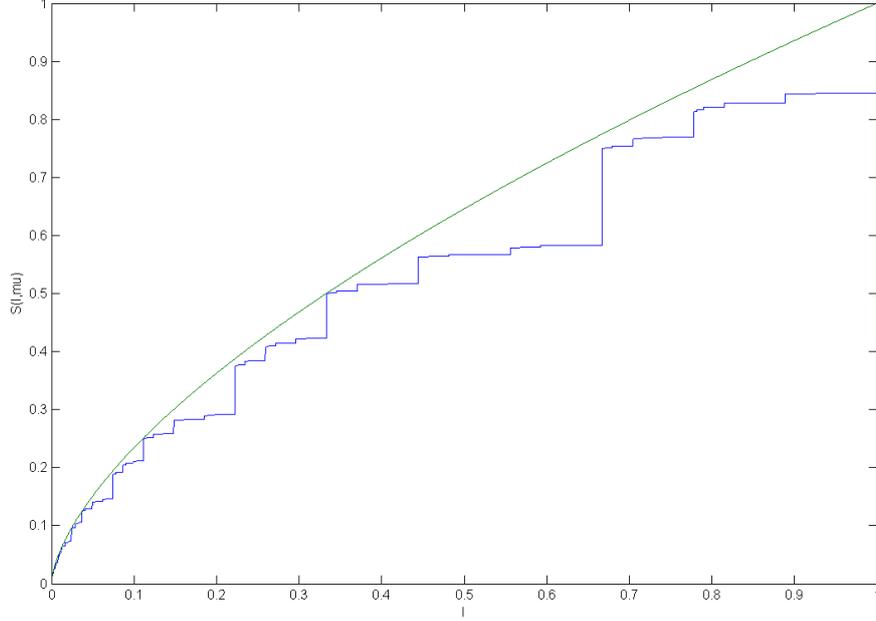
Figure 15: Blue : graph $S(l, \mu)$, surface of the Cantor dust located between the two red strips of fig . Green : graph of $l \to l^{\ln(2)/\ln(3)}$.

$$\frac{dS(l,\mu)}{dl} = \sum_n \left[\frac{s - s_n}{1 - \frac{3^{1-s}}{2}} l^{-s} \gamma(s) \right]_{s=s_n}$$
$$= \frac{l^{d_K - 1}}{\ln(3)} \sum_n l^{\frac{2i\pi n}{\ln(3)}} \underbrace{\gamma \left(1 - d_K - \frac{2i\pi n}{\ln(3)} \right)}_{\gamma_n}$$

where we used :

$$\lim_{s \to s_n} \frac{s - s_n}{1 - \frac{3^{1-s}}{2}} = \frac{1}{\ln(3)}$$

and with $d_K = \frac{\ln(2)}{\ln(3)}$ and

$$\gamma_n = \int_{K \times K} |x - y + 2|^{-d_K - \frac{2i\pi n}{\ln(3)}} d\mu(x) d\mu(y)$$

Note that the integrated area $S(l, \mu)$ is a scaling function : $S(l, \mu) = 2S(l/3, \mu)$ (see fig. (15)).

5.4 Properties of the functions $h_k(t)$

We study here the functions :

$$h_k(t) = \int_K x^k e^{-ixt} d\mu(x)$$

25

First, there is a recurrence relation verified by the $h_k(t)$:

$$h_k(t) = \int_K e^{-i\epsilon t} \epsilon^k d\mu$$

$$= \frac{3^{-k}}{2} \int_K e^{-i\epsilon t/3} \epsilon^k d\mu + \frac{3^{-k} e^{-i2t/3}}{2} \int_K e^{-i\epsilon t/3} (\epsilon + 2)^k d\mu$$

$$= \frac{3^{-k}}{2} h_k(t/3) + \frac{3^{-k}}{2} e^{-i2t/3} \sum_{j=0}^{k} \binom{k}{j} h_j(t/3) 2^{k-j}$$

From this relation, we can show by recurrence that the zeroes of $h_k(t)$ is the set :

$$Z_k = \{t_{m,k} = \frac{\pi}{2}(2m+1)3^{k+1}, m \in \mathbb{Z}\}$$

Thus, the zeroes of $h_k(t)$ are those of $h_{k-1}(t/3)$, as illustrated in fig. (16). Moreover, the $h_k(t)$ all have local maxima at points of the form $m_{n,l} = n\pi 3^l$. It was not proven rigorously for $k > 0$ (the case $k = 0$ is straightforward, the detail is given in annexe), but the numerics support this assumption and one can intuitively understand why it is so from the definition of $h_k(t)$:

$$h_k(t) = \int_K x^k e^{-ixt} d\mu = \lim_{n \to \infty} \frac{3^n}{2^n} \sum_{a_{j_n} \in K_n} \int_{a_{j_n}}^{a_{j_n} + 3^{-n}} x^k e^{-ixt} dx$$

$|h_k(t)|$ is maximal at points t such that the phase e^{-ixt} varies as little as possible as x goes through K. K is composed of real numbers which have only 0 and 2 in there decomposition in base 3, e.g. $x = \sum_{k \leq 1} \frac{\beta_k}{3^k}$ with $\beta_k \in \{0,2\}$. Now, for $t = n\pi 3^l$, we see that for any $x \in K$ whose decomposition in base 3 has only 0 after the l first terms, we have $e^{-ixt} = 1$: the phase does not change.

At these local maxima, the amplitude of the functions $h_k(t)$ decreases with k (as a consequence of Riemann-Lebesgue theorem).
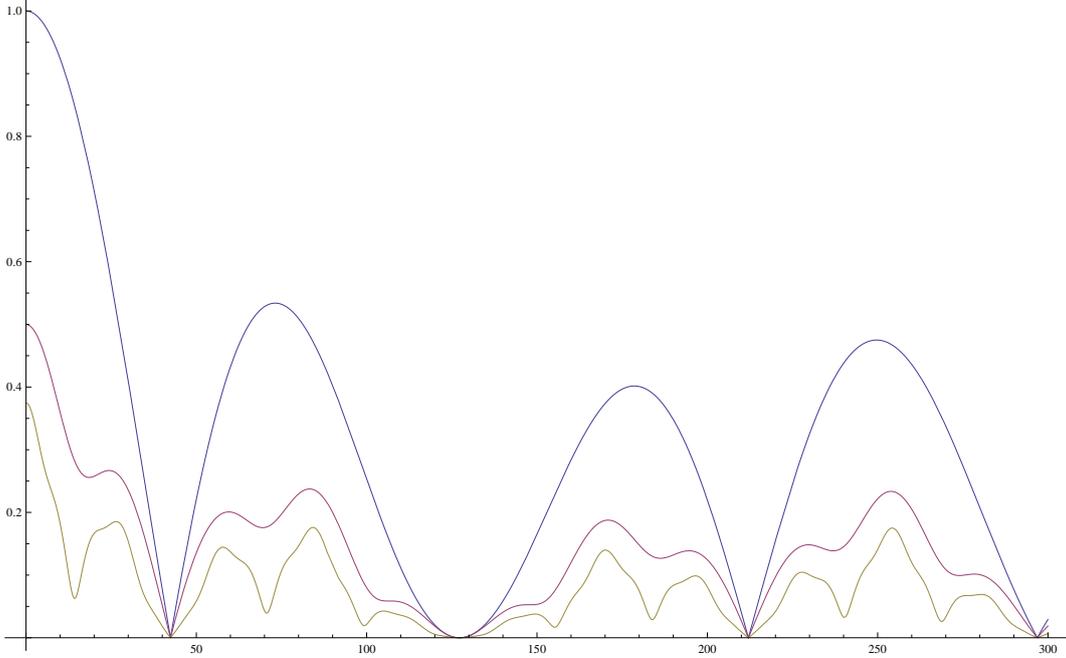

Figure 16: Numerical curves of $|h_0(t/9)|$ (blue), $|h_1(t/3)|$ (red) and $|h_2(t)|$ (yellow).

6 References

[1] Tanese, E. Gurevich, A. Lemaıtre, E. Galopin, I. Sagnes, A. Amo, J. Bloch, E. Akkermans, arxiv:1311.3453, 2013

[2] J. Feder, "Fractals", Plenum Press - New York and London, 1988

[3] E. Akkermans, O. Benichou, G. Dunne, A. Teplyaev and R. Voituriez, Phys. Rev. E 86, 061125 (2012).

[4] For a recent review, E. Akkermans, Contemporary Math- ematics 601, 1-22 (2013), arXiv:1210.6763.

[5] R. Ketzmerick, K. Kruse, S. Kraut, T. Geisel, arXiv:cond-mat/9611006v2 (1997)

[6] R. Ketzmerick, G. Petschel, and T. Geisel, Phys. Rev.Lett. 69, 695 (1992)

[7] F. Wegner, Z. Physik B 36, 209-214 (1980)

[8] B. Simon, Advances in Applied Math. 3, 463-490 (1982)

[9] D. Thouless, J. Phys. C5 (1972), 77

[10] P.J. Grabner , H. Prodinger, Statistics & Probability Letters 26 (1996) 243-248

[11] Guarneri, "Spectral Properties of Quantum Diffusion on Discrete Lattices", Eurquhys. Lett., 10 (2), pp. 95-100 (1989)

[12] C. Janot, "Quasicristals, a primer", Carendon press Oxford, 1994

[13] H. Hiramoto, M. Kohmoto, International Journal of Modern Physics B, Vol. 6, Nos 3 & 4 (1992) 281-320

[14] E. Akkermans, E. Gurevich "Spontaneous emission from a fractal vacuum",EPL, 103 (2013) 30009

[15] D. Bessis, J. D. Fournier, G. Servizi, G. Turchetti, S. Vaienti, Phys. Rev. A, Vol. 36, number 2, July 15, 1987